Properties of electron insulating phase in Si inversion layers at low temperatures

V. T. Dolgopolov, G. V. Kravchenko, and A. A. Shashkin
Institute of Solid State Physics RAS, 142432, Chernogolovka, Moscow District, Russia

S. V. Kravchenko
Institute for High Pressure Physics, 142092, Troitsk, Moscow District, Russia

(Submitted 7 May 1992)
Pis'ma Zh. Eksp. Teor. Fiz. **55**, No. 12, 701–705 (25 June 1992)

Phase boundary in the H, N_s plane has been found for the metal–insulator transition in Si inversion layers in magnetic fields normal and parallel to the interface. Transport properties of an insulating phase have been investigated. These properties are qualitatively the same, regardless of the value and the direction of the magnetic field.

The metal–insulator transition in a 2D electron gas of Si metal-oxide-semiconductor structures (MOSFET's) was investigated in detail in a number of experiments at temperatures $T > 1$ K (see Ref. 1). The results of experiments in the absence of the magnetic field were interpreted as the Anderson localization in a 2D electron system.[2] Some doubts in this interpretation have recently arisen. New features in the behavior of an insulating phase have been found in recent experiments at lower temperatures.[3] First, as the temperature decreases, the current-voltage characteristics become strongly nonlinear. At high currents (>1 nA), the voltage tends to saturate. Second, ac voltage generation was observed in the nonlinear region of the I–V characteristics. It was stated in Ref. 3 that these effects contradict the model of single-particle conduction and support the formation of a pinned quantum electron solid.

In the pioneering works[4,5] it was shown that normal magnetic field promotes an insulating phase. Competition between the integer quantum Hall effect (QHE) and the insulating phase was observed in high-mobility Si MOSFET's at low temperatures.[6]

The results mentioned above are similar to those obtained on AlGaAs/GaAs heterostructures in a quantizing magnetic field: i) At small filling factors an insulating phase which is interrupted by a fractional QHE state has been observed.[7–14] ii) The current-voltage characteristics of the insulating phase are strongly nonlinear.[10,12–14] iii) At high currents it is possible to observe a noise signal.[13] In the majority of studies the Wigner crystal is assumed to be the origin of the effects.

Another interpretation has been advanced as a result of studying the phase boundary between the metal and the insulator in the H, N_s plane for 2D electron gas in Si MOSFET's.[15] (We assume that a 2D electron system, which is capable of conducting a current in a weak electric field at zero temperature is a *metal*. In accordance with this definition, the system with zero conductivity σ_{xx} and quantized value of σ_{xy} is a metal. In an insulating phase all the components of a conductivity tensor are equal to zero at $T=0$.) This phase boundary was found to be a straight line in the extreme quantum limit. The slope of this line is $\partial N_s/\partial H \approx 1/2(e/hc)$, which presumably points to the percolation nature of the metal–insulator transition.

In the present work we have investigated the properties of an insulating phase of a 2D electron gas in Si MOSFET's: i) Phase boundary in the H, N_s plane between the metal and the insulator in the normal and parallel magnetic fields; ii) current-voltage characteristics of the insulating phase at different temperatures.

Measurements were made on three Si MOSFET's from different wafers. The peak mobilities were $\mu_{\text{peak}} \sim 3\times10^4$ cm^2/Vs at a temperature $T = 1.3$ K. All samples were of the "Hall-bar" geometry (0.25×2.5 mm^2 and 0.8×5 mm^2) with distances between the nearest potential probes 0.625 mm and 1.25 mm, respectively. The results obtained for different samples were qualitatively similar.

Measurements were carried out in a TLM-400 dilution refrigerator, with a base temperature of $\approx$25 mK. To achieve maximum mobility, the samples were slowly (for 5 h) cooled from room temperature to $T = 1.3$ K, with a fixed voltage $V_g = 10$ V between the gate and the 2D layer. This procedure enabled us to obtain the most homogeneous distribution of electrons. When measuring the temperature dependences, the temperature at every point was stabilized in order to avoid the presence of temperature gradients in the mixing chamber. We obtained current-voltage characteristics by measuring the potential difference, V, between the voltage probes when sweeping the source-drain current, I_{sd}. At temperatures below 1.3 K and at low electron densities, the contact resistances increased to very high values, so that measure-

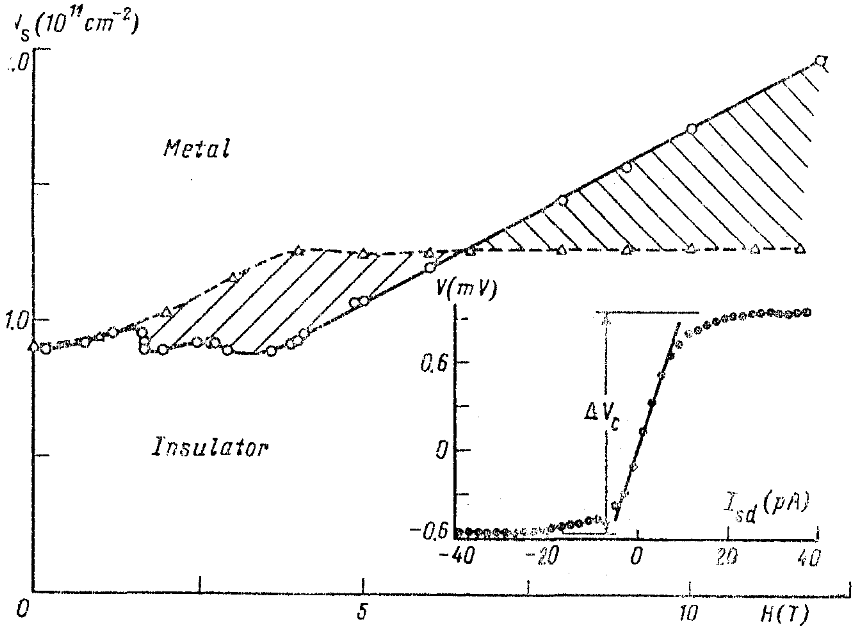

FIG. 1. Phase boundaries at parallel (triangles) and normal (dots) magnetic fields. The inset shows the I–V characteristics measured at $H = 14$ T, $T = 60$ mK, and $N_c - N_s = 0.77\times10^{10}$ cm^{-2}.

ments with a standard lock-in technique were no longer possible. All experimental results were obtained by a four-terminal dc technique using two KEITHLEY 614 DVM's as high-input-resistance preamplifiers. As in the case of low N_s, the resistance exceeded 10 GΩ, and the source-drain current was set via a resistance of 150 GΩ.

The phase diagram including low magnetic fields is shown in Fig. 1. A line separating the metal phase from the insulator phase was drawn through the points at which the longitudinal resistivity was equal to 100 kΩ. The phase boundary determined in this way is nearly independent of the temperature. In the case of a normal magnetic field (the dots in Fig. 1), it is in agreement with the results of two recent studies.[6,15] In Fig. 1 we also show a phase boundary for the same sample in a parallel magnetic field (the triangles). At high magnetic fields ($H > 4$ T) the threshold electron density was found to be constant. In a weak magnetic field ($H < 1.5$ T) it does not depend on the orientation of the magnetic field. At $H = 6.5$ T, the phase boundaries intersect each other; i.e., change in the magnetic field direction from parallel to normal causes the number of localized electrons to decrease at lower magnetic fields and to increase in the opposite case (see the hatched regions in Fig. 1).

The inset in Fig. 1 shows the current-voltage characteristics of the insulating phase. The I–V characteristics have a particular shape: At low currents the voltage is proportional to the current, while at high currents, >0.1 nA, we observe a saturation of the voltage across the sample. The shape of the I–V characteristics is the same, regardless of the location of the points in the H, N_s plane and the direction of the

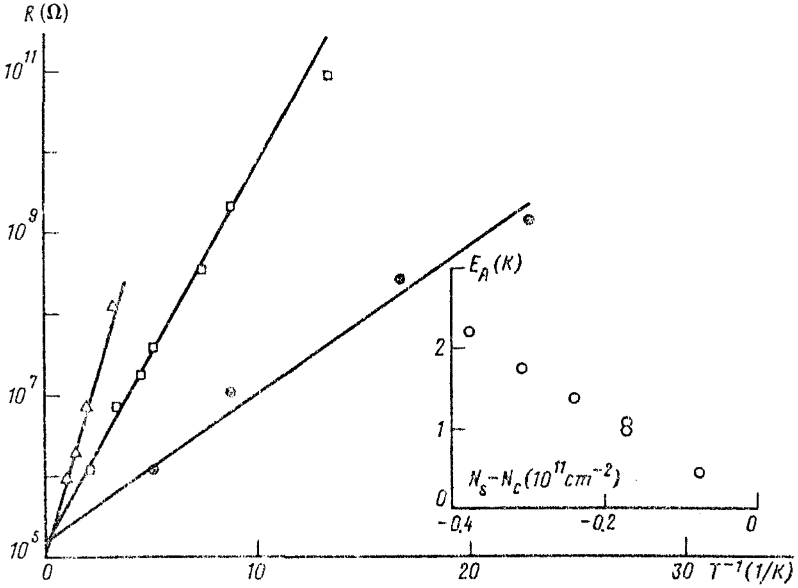

FIG. 2. The Arrhenius plots of the resistance of the linear part of the I–V curve. $H = 14$ T, $N_c - N_s = 0.77\times10^{10}$ cm^{-2}; 1.73×10^{10} cm^{-2}; 3.77×10^{10} cm^{-2}. Activation energy vs electron density is shown in the inset.

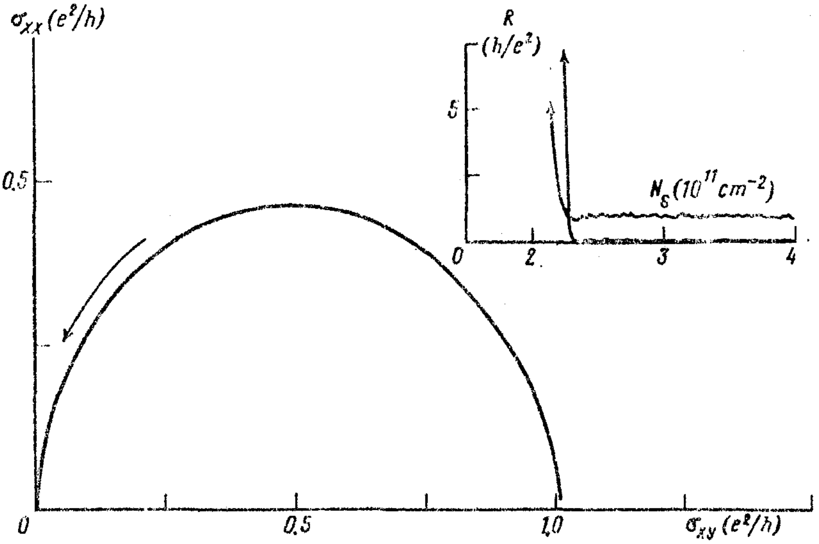

FIG. 3. The dependence $\sigma_{xx}(\sigma_{xy})$ for the lowest quantum level. The experimental dependences of the resistivities on the electron density, obtained in the region of metal–insulator transition at $H = 14$ T, are shown in the inset.

magnetic field. However, when departing from the phase boundary, the range of currents in which the I–V characteristic is linear becomes smaller and the difference ΔV_c between the threshold voltages (see the inset in Fig. 1) increases in accordance with an superlinear law. The temperature dependences of the slope of the linear part of the I–V characteristics are shown in Fig. 2 for different electron densities. These temperature dependences obey the Arrhenius law; the activation energy increases with decreasing electron density at a fixed magnetic field (the inset in Fig. 2). The absence of a jump in the activation energy at the phase boundary indicates that this transition is not a first-order phase transition. As can be seen from Fig. 2, the pre-exponential factors in the temperature dependence of the resistance are the same, suggesting that the sample is "ideal" according to Ref. 1.

The long-range potential fluctuations are assumed to be absent in the "ideal" samples.[1]

From Refs. 16 and 17 it is expected that in the σ_{xy}, σ_{xx} plane there exists a line (a separatrix) which separates the regions with a different behavior of conductivities when scaling the sample size. At sufficiently low temperature the experimental dependence of σ_{xx} on σ_{xy} should correspond to the separatrix. Figure 3 shows a part of this dependence at $\sigma_{xy} \leqslant e^2/h$, when only one quantum level is filled with electrons. The separatrix was found in the region of the metal–insulator transition; experimental curves used for calculating the conductivities are shown in the inset in Fig. 3. The shape of the separatrix is similar to that obtained in Ref. 18 at larger values of σ_{xy}, but the maximum value of σ_{xx} is three times larger.

In Ref. 19 the dependence $\sigma_{xx}(\sigma_{xy})$ was measured when the electron density slightly exceeds the electron density at the phase boundary in the absence of a magnetic field. As the filling factor decreases, a part of the experimental curve starting at the point (2,0) tends to the point (0,0) along an arc in the σ_{xy}, σ_{xx} plane. Upon further decrease of the filling factor, the curve emerges from the point (0,0) and enters the point (1,0), tracing a smaller arc. In our samples we observed an analogous behavior in the region of oscillations of the phase boundary (Fig. 1). It should be emphasized that this behavior points out the disappearance of the extended states of the completely filled lower Landau level and then their re-entrance, as the number of electrons at the upper Landau level decreases.

As was mentioned above, there are three types of metal–insulator transitions: i) the Anderson localization in a short-range potential; ii) the percolation transition in a long-range potential; iii) the formation of a Wigner electron solid. Unfortunately, the obtained experimental results do not allow us to determine unambiguously which mechanism actually takes place.

We thank V. F. Gantmakher for a useful discussion of this paper.

[1] T. Ando, A. B. Fowler, and F. Stern, Rev. Mod. Phys. **54**, 437 (1982).
[2] N. F. Mott, M. Pepper, S. Pollitt *et al.*, Proc. Roy. Soc. A **345**, 169 (1975).
[3] S. V. Kravchenko, V. M. Pudalov, J. Campbell, and M. D'Iorio, Pis'ma Zh. Eksp. Teor. Fiz. **54**, 528 (1991) [*sic*].
[4] S. Kawaji and J. Wakabayashi, Solid State Commun. **22**, 87 (1977).
[5] M. Pepper, Phil. Mag. B **37**, 83 (1978).
[6] M. D'Iorio, V. M. Pudalov, and S. G. Semenchinsky, Phys. Lett. A **150**, 422 (1990).
[7] R. L. Willett, H. L. Stormer, D. C. Tsui, L. N. Pfeiffer, K. W. West, and K. W. Baldwin, Phys. Rev. B **38**, 7881 (1988).
[8] V. J. Goldman, M. Shayegan, and D. C. Tsui, Phys. Rev. Lett. **61**, 881 (1988).
[9] E. Y. Andrei, G. Deville, D. C. Glattli, F. I. B. Williams, E. Paris, and B. Etienne, Phys. Rev. Lett. **60**, 2765 (1988).
[10] R. L. Willett, H. L. Stormer, D. C. Tsui *et al.*, Phys. Rev. B **40**, 6432 (1989).
[11] H. W. Jiang, R. L. Willett, H. L. Stormer *et al.*, Phys. Rev. Lett. **65**, 633 (1990).
[12] V. J. Goldman, M. Santos, M. Shayegan, and J. E. Gunningham, Phys. Rev. Lett. **65**, 2189 (1990).
[13] F. I. B. Williams, P. A. Wright, R. G. Clark *et al.*, Phys. Rev. Lett. **66**, 3285 (1991).
[14] H. W. Jiang, H. L. Stormer, D. C. Tsui, L. N. Pfeiffer, and K. W. West, Phys. Rev. B **44**, 8107 (1991).
[15] V. T. Dolgopolov, G. V. Kravchenko, and A. A. Shashkin, Pis'ma Zh. Eksp. Teor. Fiz. **55**, 146 (1991) [JETP Lett. **55**, 140 (1991)].
[16] H. Levine, S. B. Libby, and A. M. M. Pruisken, Phys. Rev. Lett. **51**, 1915 (1983).
[17] D. E. Khmelnitskii, Pis'ma Zh. Exp. Teor. Fiz. **38**, 454 (1983) [JETP Lett. **38**, 552 (1983)].
[18] V. T. Dolgopolov, A. A. Shashkin, B. K. Medvedev, and V. G. Mokerov, Zh. Eksp. Teor. Fiz. **99**, 201 (1991) [Sov. Phys. JETP **72**, 113 (1991)].
[19] S. V. Kravchenko, J. A. A. J. Perenboom, and V. M. Pudalov, Phys. Rev. B **44**, 13513 (1991).

Translated by the authors